Icarus **144**, 89–98 (2000)
doi:10.1006/icar.1999.6277, available online at http://www.idealibrary.com on IDEAL®

Dust Grains around Jupiter—The Observations of the Galileo Dust Detector

Kai-Uwe Thiessenhusen

Institut für Physik, Universität Potsdam, Postfach 601553, D-14115 Potsdam, Germany
E-mail: kai@agnld.uni-potsdam.de

Harald Krüger

Max-Planck-Institut für Kernphysik Heidelberg, Saupfercheckweg 1, D-69117, Heidelberg, Germany

Frank Spahn

Institut für Physik, Universität Potsdam, Postfach 601553, D-14115 Potsdam, Germany

and

Eberhard Grün

Max-Planck-Institut für Kernphysik Heidelberg, Saupfercheckweg 1, D-69117, Heidelberg, Germany

Received May 27, 1999; revised September 27, 1999

We analyze the data of the Galileo dust detector system (DDS) with respect to micrometer-sized dust grains in the inner jovian system. The analysis of these data requires an in-depth modeling because an exact determination of the orbits of individual particles directly from the data is not possible. We find that a ring of prograde particles with masses between 10^{-12} and 10^{-11} g is compatible with the data. The number density in the region around Europa's orbit is at least 4×10^{-13} cm^{-3}. The strongest impacts observed, however, are caused by a smaller population of particles in the same mass range but on retrograde orbits. These particles are probably captured interplanetary or interstellar grains (J. E. Colwell *et al.* 1998, *Science* 280, 88). Possible sources for the prograde dust are the Galilean satellites, especially Europa and Io.

Key Words: **interplanetary dust; planetary rings, Jupiter; Jupiter, magnetosphere.**

1. INTRODUCTION

During several passages through the jovian system, the dust detector system (DDS) (Grün *et al*. 1992) onboard Galileo recorded many dust impacts (Grün *et al*. 1997). The data of the DDS do not allow an exact determination of the impact direction of each individual particle. The mean impact direction of certain identifiable subgroups of particles, however, can be determined, and a range of allowable orbital parameters can be assigned to each such subgroup.

With such methods, the so-called stream particles which are responsible for the vast majority of the dust impacts observed by Galileo have been studied in previous works. These 10-nm-sized particles escape from the jovian system with very large velocities (Grün *et al*. 1997, 1998, Horanyi *et al*. 1997, Zook *et al*. 1997). Io has been suggested to be the source for these particles (Horanyi *et al*. 1993a,b) as recently could be confirmed from the Galileo data (Graps *et al*. 1999). In this paper we discuss the impact events of larger, about micrometer-sized, particles. Colwell *et al*. (1998) have shown that a number of these impacts cannot be explained by particles on prograde circular orbits. They suggested a capture mechanism for interplanetary or interstellar micrometer-sized particles in the jovian magnetosphere. This mechanism provides orbits with low eccentricities and low inclinations, and about 80% of them are retrograde.

However, at the time of these studies, only a very small number of impacts onto the DDS had been available. Meanwhile, many more large impact events have been recorded. The understanding of their nature can help in obtaining new information about the dust environment of Jupiter.

This paper is organized as follows: in the next section, we discuss the data structure and the information contained therein and the geometry of the detection process. The third section describes the analysis of the data. Constraints on the dust distribution around Jupiter are given in the fourth section. Finally we summarize our results.

2. DATA AND ORBITAL GEOMETRY

The DDS on Galileo is an impact ionization detector. A dust grain hitting the detector causes an ionization signal on the

0019-1035/00 $35.00

sensitive target. The signal amplitude depends on the mass and speed of the particle. From Earth-bound calibration experiments, an empirical relation between the signal intensity (ionization charge Q) and the mass m of a grain and the impact speed v has been obtained (Grün *et al*. 1992, 1995a),

$$Q \propto m^a \cdot v^b, \tag{1}$$

with the exponents $a \approx 1$ and $b \approx 3.5$.

For convenience, the signal intensities have been classified into six amplitude ranges (AR), each of which corresponds roughly to one order of magnitude in impact charge. The majority of impact signals are in the lowest amplitude range (AR = 1), mostly caused by the stream particles mentioned above. In this paper, we consider only the stronger impacts with AR $\geq$ 2. Nearly all of them are in the amplitude ranges 2, 3, and 4; only very few AR = 5 and AR = 6 impacts have been observed in the inner jovian system.

In addition, the impact events are separated into four quality classes (CLN) (Grün *et al*. 1992). CLN = 3 events have always been considered as real dust events (Grün *et al*. 1995b, 1997, 1998). In the inner jovian system, a number of CLN = 2 impacts (and the majority of those in the two lowest quality classes CLN = 1 and CLN = 0) are contaminated with noise (Grün *et al*. 1997, Krüger *et al*. 1999a,b). Krüger *et al*. (1999b) showed that for impacts in AR = 1 the field of view and the effective detector area for CLN = 2 differs from that of CLN = 3. Therefore, for the investigation of the individual impact characteristics, we put our main attention on the CLN = 3 impacts. For statistical analysis, however, it is necessary to consider the CLN = 2 impacts too.

The detector rotates around an axis which usually points away from Earth. The axis of the detector is tilted away from this spin axis by an angle of 60° (Krüger *et al*. 1999a; in previous literature an erroneous value of 55° has been used). The position of the detector with respect to the spin axis, i.e., the so-called rotation angle ROT, is recorded for each impact. This value gives the only direction information recorded in the data. (Note that the direction of increasing ROT is opposite to the spin direction of the spacecraft (Grün *et al*. 1995b)). ROT = 0 is the direction closest to the ecliptic North. Particles coming from close to the ecliptic plane will be detected either from ROT $\approx$ 270° or ROT = 90°. Because it is not possible to determine from where in the 140° cone of the detector a particle impacts, there is a systematic uncertainty of $\pm$70° in the measured ROT values.

As an example, Galileo's trajectory for the Callisto 3 (C3) encounter is plotted in Fig. 1 (left). Earth is in the positive x direction; the spin axis of Galileo points to the negative x direction (see the inset in Fig. 1, left). Galileo itself has a prograde eccentric orbit. Therefore, close to its perijove, its speed is larger than for particles on circular Keplerian orbits.

In the right part of Fig. 1, the observed rotation angles of all particles recorded during the C3 encounter have been plotted as a function of time (in days of the year 1996). It is obvious that the larger impacts (asterisks and crosses) have different characteristics in comparison with the weaker AR = 1 impacts (dots). One typical effect is the shift of ROT for the stream particles around day 309. Then the particles impact from the direction of the spin axis (anti-Earth direction, see below). At this time the direction of a stream is known directly from the measurements.

Nearly all impacts have been detected from ROT = 270 $\pm$ 70° or ROT = 90 $\pm$ 70°, i.e., from close to the ecliptic plane. Therefore we put our main attention on particles impacting from the ecliptic plane and define there the impact angle ϕ as the angle between the vector of relative speed of an impacting particle and Galileo's spin axis (Fig. 2, left). This means that particles with $\phi = 0$ impact from the direction of the spin axis (opposite to

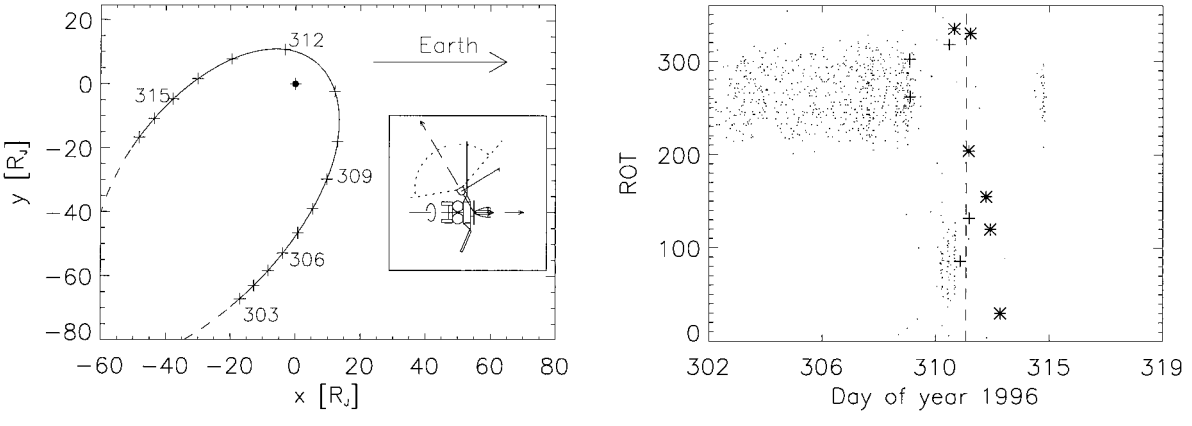

FIG. 1. (Left) Orbit of Galileo during the Callisto 3 (C3) encounter in a cartesian coordinate system with Jupiter in the origin. The lengths are given in jovian radii. Earth is in the positive x direction. (Inset) The orientation of Galileo. Its spin axis points into the negative x direction (opposite to Earth). The rotation angle ROT of Galileo is measured increasingly positive (seen from Earth), opposite to the direction of the spacecraft rotation. ROT = 0 is the direction closest to the ecliptic North. The orientation of the sensor is displayed here for a rotation angle of 270°. The sensor axis (dashed line) and the limits of the field of view (dotted lines) are plotted. (Right) Measured rotation angles of the dust events detected during this encounter as a function of time (in days of the year 1996). All events in the highest significancy class CLN = 3 are displayed. The dots denote impacts in the lowest amplitude range AR = 1, crosses AR = 2, and asterisks AR $\geq$ 3 impacts. The dotted vertical line denotes the time of Galileo's perijove passage.

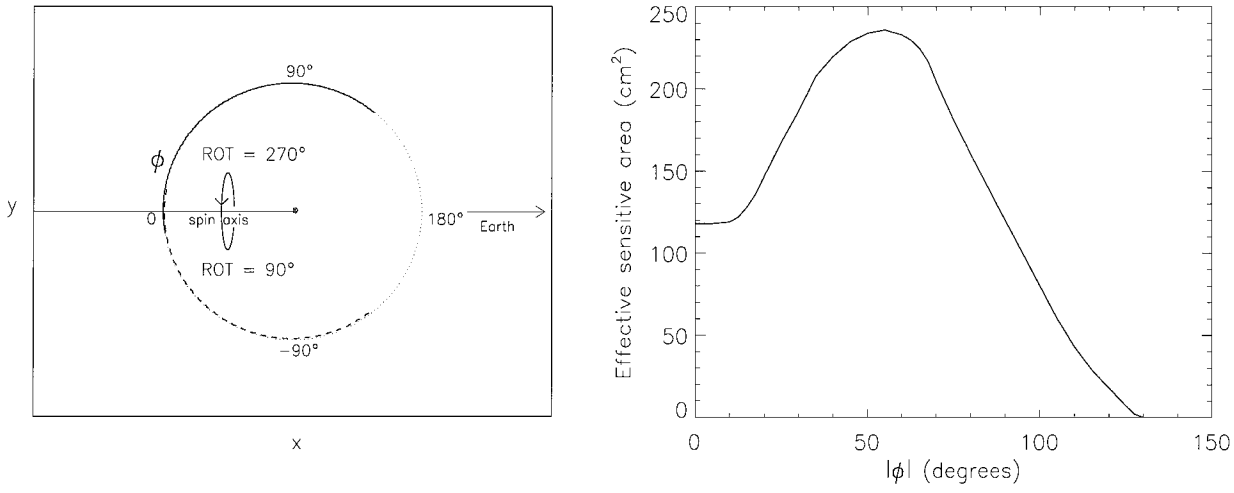

FIG. 2. Detection geometry. (Left) The impact angle ϕ is the angle between the vector of impact speed of a particle and Galileo's spin axis (left) which points away from Earth. The solid line shows the field of view for a rotation angle ROT $= 270°$ and the dashed line for ROT $= 90°$. The orientation is the same as in Fig. 1 (left). (Right) Effective sensitive area (in cm^2) of the Galileo dust detector averaged over one rotation period of the spacecraft as a function of the absolute amount of the impact angle $|\phi|$.

Earth). Note that this orientation does not depend on Galileo's motion around Jupiter.

The relation between the observed rotation angle ROT and the impact angle ϕ is as follows: particles will be detected from ROT $\approx 270°$ when $\phi > 0$ (solid line in Fig. 2, left) and from ROT $\approx 90°$ for $\phi < 0$ (dashed line). With respect to Fig. 1 (left), this means that particles with a negative *y* component of relative speed have $\phi > 0$, and vice versa. Particles impacting from close to the spin axis ($|\phi| < 10°$) can be observed from all rotation angles; particles impacting from $|\phi| > 130°$ are always out of the field of view of the detector.

The relation between ϕ and the effective sensitive area A_S of the detector is plotted in Fig. 2 (right). The total sensitive area A_0 of the detector is 1000 cm^2. However, the effective area which is available for the detection of a particle is always smaller due to the rotation of the detector and the angle between the relative velocity vector and the direction of orientation of the sensor.

The maximum value of A_S (averaged over one rotation period) is about 235 cm^2 for $|\phi| \approx 55°$ (Krüger *et al*. 1999b, see also Grün *et al*. 1992). For smaller values of $|\phi|$, A_S reduces to about 120 cm^2 at $\phi = 0$. For larger $|\phi|$, A_S decreases monotonously down to zero for $|\phi| \approx 130°$.

3. DATA ANALYSIS

Figure 3 displays the recorded large AR ≥ 3 (asterisks; nearly all of them are in the amplitude ranges 3 and 4) and AR $= 2$ (crosses) CLN $= 3$ impact events from the first 15 passages of Galileo through the inner jovian system. In these regions, the Galileo DDS data in the studied amplitude ranges can be considered to be complete, withouts gaps in the recording.

Obviously, the vast majority of impacts has been detected within 2 days around Galileo's perijove passages, i.e., inside 20 jovian radii, R_J. Further outside, the impact rate is much smaller. At the studied encounters, Galileo's perijove distances were between 8.8 and 11R_J from Jupiter. No *in situ* measurements of the dust population further inside were possible.

There are several differences between the stronger and less strong impacts: Several AR $= 2$ but almost no AR ≥ 3 impacts have been observed more than 1 day before the perijove passages. The measured rotation angles ROT also show different characteristics for AR ≥ 3 and AR $= 2$ impacts, respectively: after about 1 day after the perijove passages, nearly all AR ≥ 3 impacts have ROT $\approx 90°$. In contrast, the majority of the AR $= 2$ is observed from ROT $\approx 270°$ at the same time. Before this time,

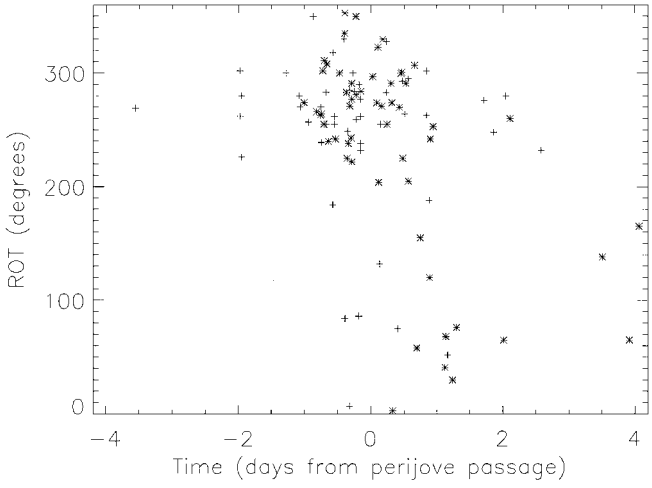

FIG. 3. Measured rotation angles as a function of time for the AR $= 2$ (crosses) and AR ≥ 3 (asterisks) CLN $= 3$ impacts from the first 15 passages of Galileo through the inner jovian system (June 1996–May 1998). The time is given in days from Galileo's perijove passage.

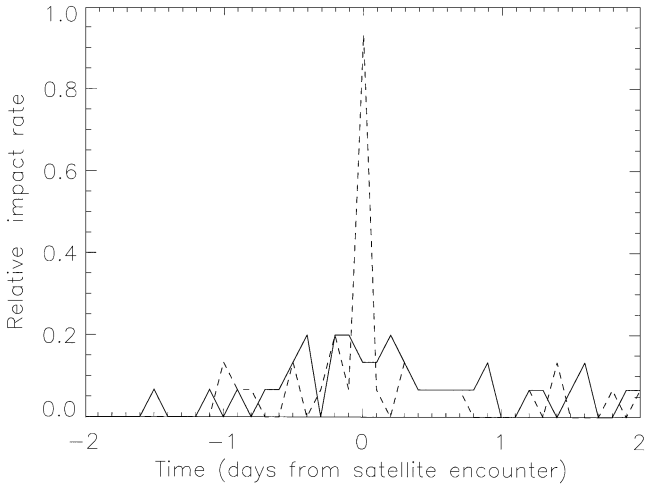

FIG. 4. Impact rates (events per day) versus time (in days) from Galileo's closest encounters with the Galilean satellites for AR = 2 (dotted line) and AR = 3 (solid line) impacts. The rates are calculated in 0.1-day intervals. Note that the time scale here differs from that in the other images.

AR ≥ 3 as well as AR = 2 impacts have ROT ≈ 270°, except for a fraction of AR = 2 recorded from smaller rotation angles close to Galileo's perijove passages. We will discuss these effects later.

There is another observable difference between these two groups: Nearly all passages of Galileo include a close encounter with one of the Galilean satellites. Such satellites can be expected to be a source of dust (Krüger *et al*. 1999c). This leads to an increased dust concentration inside their Hill spheres as seen in Fig. 4. The impact rates of the AR = 2 events (dashed line) show a strong increase close to the encounters with the Moon. Only a weak increase can be observed for AR ≥ 3 events (solid line).

Almost one-third of the AR = 2 impacts have been recorded in the close vicinity of the Galilean satellites within 1 h of the closest encounter with the Moon. We exclude these events from our further considerations.

As pointed out above, an exact determination of the impact direction and, thus, the orbit of a particle is not possible from the data. Therefore, it is necessary to model particles on different possible orbits and to study how they would be observed by the Galileo dust detector in comparison with the measured data. Because only large particles with sizes in the order of 1 μm are discussed here, it is possible to assume for these observational conditions that the particles have nearly Keplerian orbits.

Circular Orbits

First we consider circular orbits in the equatorial plane. Figure 5 displays the evolution of the relative speed v (left), the signal intensity (middle), and the impact angle ϕ (right) for particles on retrograde (solid lines) and prograde (dashed lines) circular orbits as a function of time from Galileo's perijove. In this example, we used the orbital data of the C3 encounter of Galileo.

Close to perijove passage, the impact velocities are about three times higher for retrograde than for prograde particles. This has several consequences for the detection of dust. The measured signal intensity is very sensitive to the impact velocity (Eq. (1)). Therefore, retrograde particles cause impact signals between one and more than two orders of magnitude stronger than those of prograde impactors of the same mass. This effect gives a distinct separation of prograde and retrograde particles with the same mass. For instance, prograde particles with a mass of 10^{-12} g (typical for micrometer-sized grains) cause impacts in the amplitude ranges AR = 1 and AR = 2, retrograde of the same mass in AR = 3 or AR = 4 (Fig 5, middle). In other words, prograde impactors must have a mass orders of magnitude higher then retrograde ones to cause impact signals of the same intensity.

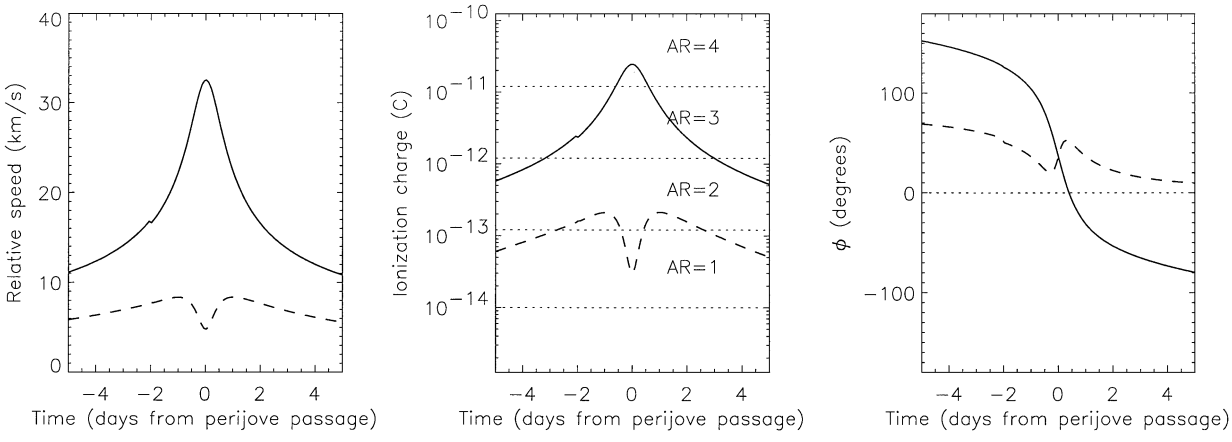

FIG. 5. Conditions for the observation of particles on prograde (dashed lines) and on retrograde (solid lines) circular orbits at the Callisto 3 encounter calculated as a function of time (in days) from Galileo's perijove passage. (Left) impact velocities; (middle) impact signal intensities for particles with masses of 10^{-12} g. The dotted lines separate the different amplitude ranges. (Right) Impact angles ϕ with respect to Galileo's spin axis. The dotted line denotes $\phi = 0$, which is connected with the shift in the measured rotation angles.

The impact angles for prograde and retrograde particles also follow different characteristics (Fig. 5, right). For prograde particles, ϕ is always positive; for retrograde particles, however, ϕ becomes negative after Galileo's perijove passage. This means that the rotation angle for the observation of retrograde particles then shifts from 270° to 90°. (A short time before and after this shift, retrograde particles can be observed from all rotation angles.) Thus, the criteria for the separation between prograde and retrograde particles are:

- Retrograde particles can be detected only from a short time before Galileo's perijove passages. They cannot be observed earlier. A shift in the rotation angle for their detection takes place a certain time after Galileo's perijove passages.
- Prograde particles are observable during the whole time of the encounter. No shift in the rotation angle can be observed for particles on prograde circular orbits.

This is studied in Fig. 6. The observed rotation angles of all large dust impact events from the first 15 encounters of Galileo are plotted. Here, the time $t = 0$ refers to the calculated time of shift of the rotation angle (i.e., $\phi = 0$, see Fig. 5, right) for retrograde particles for each encounter. Depending on the geometry of the orbits, Galileo's perijove passages take place between $t \approx -0.5$ days and $t \approx -2$. We will discuss this in detail below.

Nearly all of the observed AR $\geq$ 3 events (Fig. 6, top) are in agreement with the characteristics expected for retrograde particles. The weaker AR = 2 impacts (bottom), however, have a different characteristic. The majority of them come from 270° also for $t > 0$. This is expected for prograde particles. A few AR = 2 events have been detected for ROT $\approx 90°$ but close to the perijove passages, i.e., before the ROT shift for the observation of retrograde particles. This is not expected for particles on prograde circular or on retrograde orbits. Nearly all of these impacts had been observed at earlier encounters of Galileo. In order to understand this effect, we have to study particles on eccentric orbits.

Eccentric Orbits

For particles on eccentric or inclined orbits, the observational conditions may be different. It is obvious that the influence of deviations from a purely circular motion on impact directions and velocities is largest when the relative velocities with respect to Galileo are smallest. As we discussed above, this is the case for prograde particles detected around the perijove passages of Galileo. Figure 7 illustrates this. Impact velocities (top) and impact angles (bottom) are computed for particles on retrograde (left) and prograde (middle and right) eccentric orbits in the ecliptic plane. Their semimajor axes and eccentricities are randomly chosen within the ranges of $4R_J \leq a \leq 20R_J$ and $0 \leq e \leq 0.6$, respectively. The solid lines denote impact velocities and impact angles for particles on circular orbits.

The influence of eccentricities on retrograde orbits (Fig. 7, left) is small because of the much higher impact velocities with respect to prograde particles. Relative velocities (top left) and

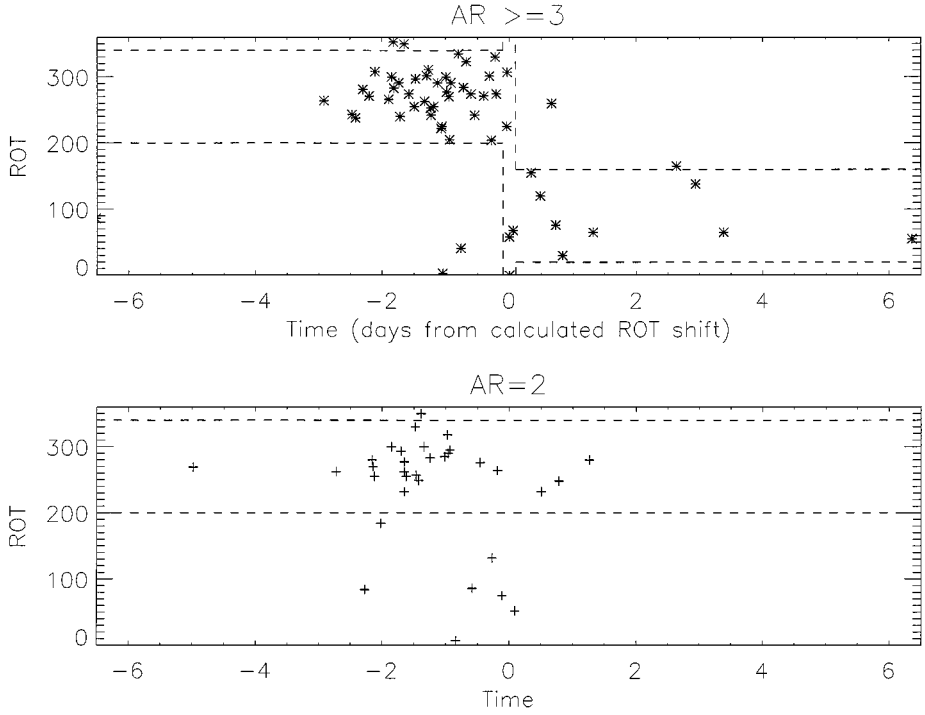

FIG. 6. Measured rotation angles for CLN = 3 impacts in the amplitude ranges AR > 3 (asterisks, top) and AR = 2 (crosses, bottom), respectively, as a function of time (in days). $t = 0$ is the calculated time of shift of the rotation angles for the observation of retrograde particles. The dashed lines denote the rotation angle range under which retrograde particles (top) and prograde particles (bottom), respectively, on circular orbits in the ecliptic plane can be observed.

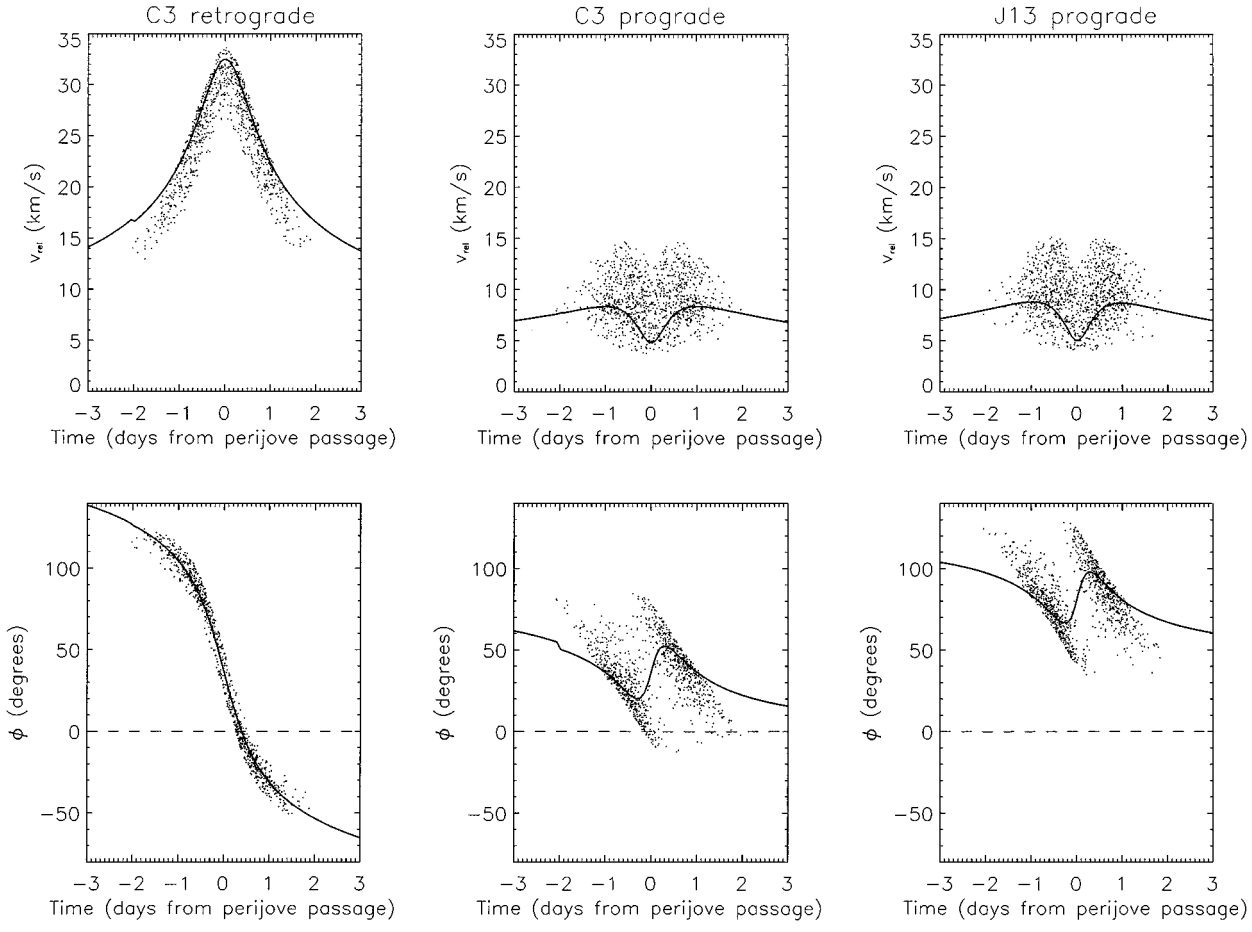

FIG. 7. Detection of particles on retrograde (left) and prograde (middle and right) eccentric orbits. The calculated impact velocities (in km/s) (top) and impact angles ϕ (in degrees; bottom) are displayed as a function of time in days from Galileo's perijove passage. The dots denote the impacts of single particles with semimajor axes randomly chosen from between 4 and 20 jovian radii and eccentricities between 0 and 0.6. As a comparison, the solid line displays the detection conditions for particles on circular orbits. Angles and velocities have been calculated for the orbit of Galileo during the C3 encounter (left, retrograde; middle, prograde particles), and for prograde particles also for the J13 encounter (right).

impact angles (bottom left) differ only slightly between particles on circular and eccentric retrograde orbits. In contrast, eccentricities influence the detection of prograde particles significantly (Fig. 7, middle and right). The relative velocities (top middle and right) of eccentric particles are on average somewhat higher than for particles on circular orbits, but the main characteristics are similar. Close to Galileo's perijove passage, the impact angles (bottom middle and right) differ significantly from those expected for circular orbits. Particles on the outward directed part of their eccentric orbits impact from angles up to 60° smaller than particles on circular orbits. The opposite effect can be observed for particles on the inward parts of their orbits.

These effects are the same for the early encounters (middle panels, C3) as well as for later encounters (right panels, J13). However, the consequences for the detection of particles are different. For particles on the outward part of their orbits there might be $\phi < 0$ at early encounters; i.e., they will be detected from ROT $\approx 90^\circ$. This, indeed, is observed in the data! There are some AR $= 2$ impacts (see Fig. 6) detected from ROT $\approx 90^\circ$ close to the time of Galileo's perijove passages. Nearly all of these events have been observed during the early encounters of Galileo. This is in agreement with the simulations: At later encounters (see Fig. 2) ϕ is larger, and it is always $\phi > 0$. On the other hand, ϕ for particles on the inward part of their motion is so large that they might be out of the field of view or impact from a direction where the effective sensitive area of the detector is rather small. This would lead to lower detection rates at later encounters (see below).

Inclinations of the orbits of the particles would lead to an observation from slightly different rotation angles. However, due to the uncertainty of each measurement of ROT of $\pm 70^\circ$, mostly only a broadening of the distribution of the measured ROT values can be an indicator for orbital inclinations. Although some impacts might be caused by particles on inclined orbits, this effect could not be studied in detail due to the small amount of available data.

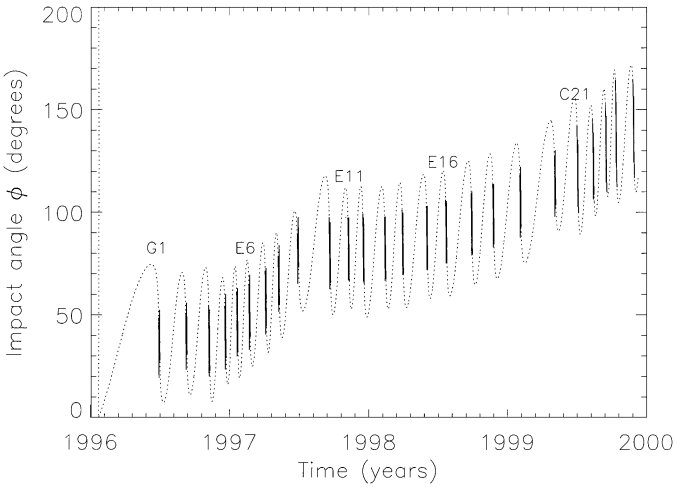

FIG. 8. Long-term evolution of the impact angle ϕ for particles on prograde circular orbits. The thick sections denote the passages through the inner jovian system within 3 days around Galileo's perijove passages. Some encounters are labeled in the image.

Influence of Changes in the Encounter Geometry

As mentioned above, the orbits of Galileo differ from encounter to encounter. The main effect of importance here is the rotation of the pericenter angle of Galileo with respect to Earth as a consequence of the orbital motion of Jupiter. This influences the observational conditions.

Figure 8 displays the evolution of the impact angle for particles on prograde circular orbits for the first 25 encounters of Galileo. $\phi > 0$ is always given. Such particles will always be detected from ROT $\approx 270^\circ$. However, ϕ increases on average from encounter to encounter. Due to the lower effective sensitive area (Fig. 2) a smaller number of prograde particles would be detected for later encounters than for earlier ones assuming a constant flux.

The characteristic properties for the detection of retrograde particles are the time when they first enter the field of view and the time of the shift of the rotation angle. These values have been plotted in Fig. 9. At later encounters, trajectories initially enter the field of view later. This means that at later encounters the number of observable retrograde particles decreases. Also, the time after Galileo's perijove passage when the rotation angle shifts increases. The majority of the particles will be observed from ROT $\approx 270^\circ$, the same angle as for prograde particles.

There are very few particles which do not follow the above characteristics. Of course, some particles observed by Galileo might have other than prograde or retrograde bound orbits around Jupiter.

4. DISTRIBUTION OF DUST

The question remains as to how the observed dust in the jovian system is distributed. It is possible to estimate radial density profiles from the data: The impact rate $\mathrm{d}N/\mathrm{d}t$ recorded by Galileo from particles from a given population is proportional to their number density n and the relation between both quantities is given by

$$\frac{\mathrm{d}N}{\mathrm{d}t} = n \cdot v \cdot A_S(\phi), \tag{2}$$

with v being the magnitude of the relative speed and $A_S(\phi)$ the effective area of the detector as a function of the impact angle ϕ (see Fig. 2); and ϕ and v depend on the orbital geometry of Galileo.

Figure 10 (left) provides the calculated relative efficiency (which is proportional to the effective sensitive area $A_S(\phi)$ and to the relative velocity v) for a dust population on circular retrograde orbits (solid line) compared to that of a prograde circular population (dashed line) for two different encounters, the C3 and the J13 encounter.

For prograde particles, the efficiency shows only a small time variability. A small drop around the perijove resulting from the reduced relative velocities is observable. In contrast, the efficiency for retrograde particles is zero when the particles impact from out of the field of view until some days before the perijove and shows a strong increase afterward. Around perijove it is about four times larger than that for prograde particles. This is valid for the early (C3 encounter, top left) as well as for later encounters (J13, bottom left).

In the middle row, the observed total impact rates from the first 15 encounters of Galileo are plotted as a function of time from the perijove passages. Up to now, we have considered events in the highest quality class CLN = 3 only in order to ensure that we analyze real dust impacts. However, the majority of the CLN = 2

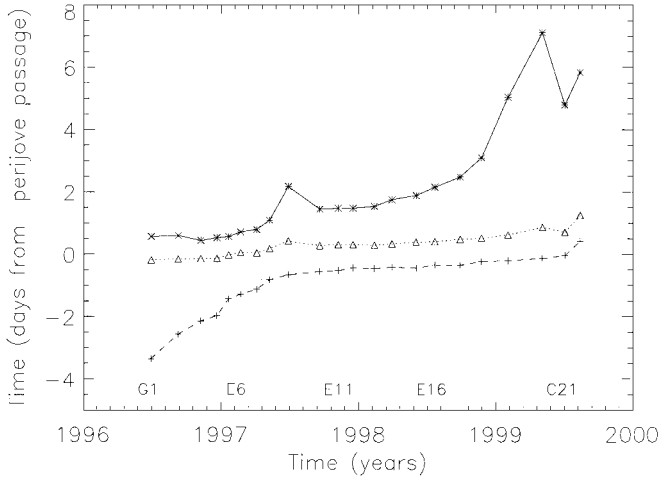

FIG. 9. Long-term evolution of the conditions of detection of retrograde particles. The lines display the time (in days) from Galileo's perijove passage when the impact angle ϕ for particles on retrograde circular orbits becomes: 0° (asterisks, solid line), i.e., the time of shift of the rotation angle for observation; 55° (triangles, dotted line), the angle when the effective sensitive area of the detector is highest; and 130° (crosses, dashed line) when the particles impact first inside the field of view of the detector.

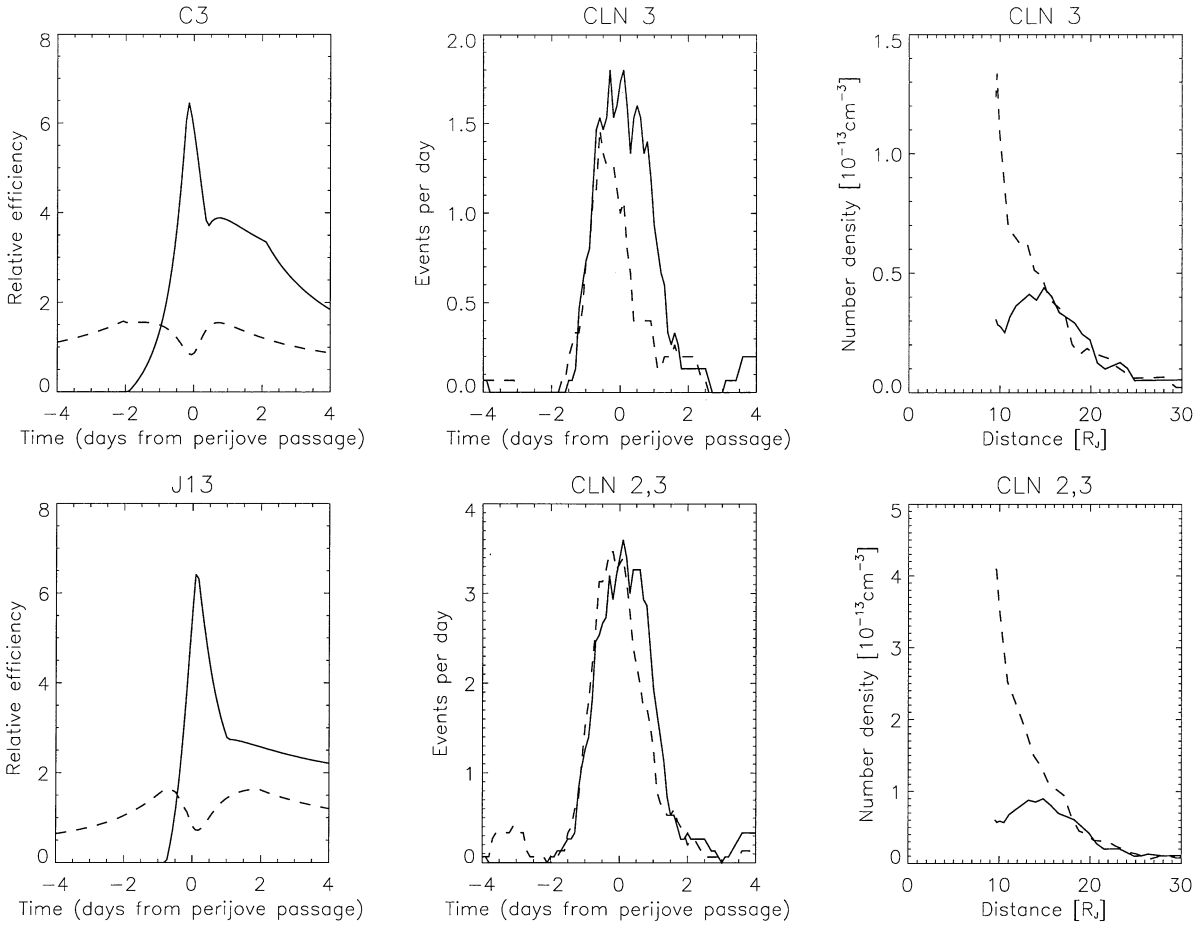

FIG. 10. (Left) Calculated relative efficiency of Galileo (in arbitrary units) for the detection of prograde (dashed line) and retrograde (solid line) particles as a function of time (in days from Galileo's perijove passage). (Top) C3; (bottom) J13. (Middle) measured impact rates per day as a function of time in days from Galileo's perijove passages. The solid line denotes AR ≥ 3, the dashed line AR $= 2$ impacts. The rates are moving averages over 1 day, averaged for the first 15 encounters of Galileo. (Top) Class 3 events only, (bottom) class 2 and 3 impacts. (Right) Radial density profiles (number density as a function of distance from Jupiter) estimated from the observed impact rates and the calculated efficiency for the first 15 encounters of Galileo. The retrograde population is marked with a solid and the prograde with a dashed line. (Top) Densities obtained only from class 3, (bottom) class 2 and 3 impact events.

events are also "real" dust events (Krüger *et al*. 1999b), so that it is necessary to take them into account for statistical purposes. We compare the rates taken from only the CLN $= 3$ events (middle row, top panel) with that from CLN $= 2$ and CLN $= 3$ together (bottom panel) for the AR $= 2$ (dashed line) and the AR ≥ 3 impact events (solid line). In both cases, the plotted rates are 1-day averages.

The impact rates for the AR ≥ 3 impacts are roughly in the same order of magnitude as for the AR $= 2$ ones. In Fig. 10 (right) we show the density profiles obtained from the calculated efficiency and the observed impact rates. Because of the fact that retrograde particles come into the field of view only a short time before Galileo's passages, we calculated the densities for the retrograde population from the impacts recorded after Galileo's perijove passages only. The density for the prograde population is averaged from the rates before and after perijove. Beside the rates, the radial positions of Galileo have also been averaged in the same interval.

The density of prograde particles significantly exceeds that of the retrograde ones. Beside this, there is a density increase with smaller distance from Jupiter for prograde particles. For retrograde particles this increase stops within about $15R_J$.

We obtain density maxima of the order of 4×10^{-13} cm^{-3} for prograde and 1×10^{-13} cm^{-3} for retrograde particles. The density profile inside $9R_J$ cannot be obtained from these *in situ* measurements. Especially for prograde particles, the number density might be still much higher inside $9R_J$. At Galileo's very first approach to the inner jovian system (Io encounter) its pericenter had been close to Io's orbit and several dust impacts had been recorded inside $9R_J$. For several technical reasons (change of the sensitivity threshold of the detector during this fly-by; gap in the observed data), these data are not suitable for a deeper analysis.

The density profile of prograde particles obtained here is a lower estimate. A number of prograde particles in the studied mass range would cause impacts only in the lowest amplitude

range AR = 1 (see Fig. 5, middle). These impacts could not be studied for two reasons: they are not recorded completely by the Galileo DDS (unlike for AR ≥ 2 impacts, a complete data set is available for only about 1/10th of the AR = 1 impacts). Beside this, the AR = 1 events are so dominated by the stream particles that it is mostly impossible to separate impacts resulting from other sources.

Therefore, we cannot give a lower limit for the mass of prograde particles from the observation. However, an upper limit can be estimated. As pointed out above, impacts of prograde particles can be clearly separated from retrograde ones by the measured rotation angles in the late stages of each encounter. Almost no AR ≥ 3 impacts follow the characteristics of prograde impactors at this time. While this might be slightly skewed by particles on eccentric orbits, we can estimate that at least the majority of prograde particles is not larger than about 10^{-11} g, and, vice versa, the majority of retrograde particles is not smaller than about 10^{-12} g. The rareness of impacts in the highest amplitude ranges 5 and 6 leads to the conclusion that 10^{-11} g would be a good estimate for the upper limit of the mass of the most of the retrograde particles, too. This is in good accordance with particles sizes of 1 μm or something less deduced by Colwell *et al*. (1998) from the capture mechanism.

The question for the sources of the dust grains remains. For retrograde particles, our estimates confirm the results from the capturing theory of Colwell *et al*. (1998). A possible source for prograde particles are the Galilean satellites. Many particles have been observed in their close vicinity (Grün *et al*. 1997, Krüger *et al*. 1999c). However, we do not observe significant density enhancements close to the orbits of Ganymede and Callisto away from the satellites itself. Therefore, the main sources could be the inner Galilean satellites Europa and Io (A. V. Krivov, pers. commun.). Information about the dust population inside Europa's orbit would help to solve the question for the origin of the observed dust. Future encounters, when Galileo will get close to Jupiter, will help to give information about this region. Unfortunately, the conditions for the observation of prograde as well as of retrograde particles become worse than at previous encounters (see Figs. 8 and 9).

5. CONCLUSIONS

In this paper we have analyzed the data of the Galileo dust detector for large, micrometer-sized dust grains. We found that there exists two different populations of such large particles. This is indicated by several differences in the observation of impacts in the largest AR ≥ 3 and the somewhat weaker AR = 2 amplitude ranges. We identified the largest AR ≥ 3 events to be mostly caused by particles on retrograde orbits, the weaker AR = 2 by particles on prograde orbits. These conclusions partially derive from the expectation that retrograde particles would cause about two orders of magnitude stronger impacts than prograde ones of the same mass.

The motion of Galileo itself significantly influences the detection process. For a given density, prograde particles would cause not only weaker but also fewer impacts than retrograde particles do. From the observations, we found that the number density of the prograde population exceeds that of the retrograde ones by at least a factor of four.

While we could confirm the order of magnitude of the density of the retrograde population proposed by Colwell *et al*. (1998), other sources, like the inner Galilean satellites Io and Europa, must be taken into account to explain the prograde population.

A number of micrometer-sized dust particles has been observed in the close vicinity of the Galilean satellites. A number of particles may be fast enough to overcome the Hill spheres of the satellites. These particles could form the dust population observed by Galileo. Because of the inward increasing density, the main sources of dust could be the inner two Galilean satellites. At future encounters of Galileo, the pericenter will be significantly closer to Jupiter than at previous ones. Therefore, data from these encounters may help explain the question for the origin of the dust.

ACKNOWLEDGMENTS

The authors thank both referees, Herb Zook and Josh Colwell, for their helpful comments and suggestions. This work has been supported by the Deutsches Zentrum für Luft- und Raumfahrt (DLR).

REFERENCES

Colwell, J. E., M. Horanyi, and E. Grün 1998. Capture of interplanetary and interstellar dust by the jovian magnetosphere. *Science* **280**, 88–91.

Graps, A. L., E. Grün, H. Svedhem, H. Krüger, M. Horányi, A. Heck, and S. Lammers 1999. Jovian dust streams origin revealed. *Nature*, submitted.

Grün, E., M. Baguhl, N. Divine, H. Fechtig, D. P. Hamilton, M. S. Hanner, J. Kissel, B.-A. Lindblad, D. Linkert, G. Linkert, I. Mann, J. A. M. McDonnell, G. E. Morfill, C. Polanskey, R. Riemann, G. Schwehm, N. Siddique, P. Staubach, and H. A. Zook 1995b. Three years of Galileo dust data. *Planet. Space Sci.* **43**, 953–969.

Grün, E., M. Baguhl, H. Fechtig, D. P. Hamilton, J. Kissel, D. Linkert, G. Linkert, and R. Riemann 1995a. Reduction of Galileo and Ulysses dust data. *Planet. Space Sci.* **43**, 941–951.

Grün, E., H. Fechtig, R. H. Giese, J. Kissel, D. Linkert, D. Maas, J. A. M. McDonnell, G. E. Morfill, G. Schwehm, and H. A. Zook 1992. The Galileo dust detector. *Space Sci. Rev.* **60**, 317–342.

Grün, E., H. Krüger, S. Dermott, H. Fechtig, A. Graps, B. A. Gustafson, D. P. Hamilton, M. S. Hanner, A. Heck, M. Horanyi, J. Kissel, B. A. Lindblad, D. Linkert, G. Linkert, I. Mann, J. A. M. McDonnell, G. E. Morfill, C. Polanskey, G. Schwehm, R. Srama, and H. A. Zook 1997. Dust measurements in the jovian magnetosphere. *Geophys. Res. Lett.* **24**, 2171–2174.

Grün, E., H. Krüger, A. Graps, D. P. Hamilton, A. Heck, G. Linkert, H. A. Zook, S. Dermott, H. Fechtig, B. A. Gustafson, M. S. Hanner, M. Horanyi, J. Kissel, B. A. Lindblad, D. Linkert, I. Mann, J. A. M. McDonnell, G. E. Morfill, C. Polanskey, G. Schwehm, and R. Srama 1998. Galileo observes electromagnetically coupled dust in the jovian magnetosphere. *J. Geophys. Res.* **103**, 20,011–20,022.

Horanyi, M., E. Grün, and A. Heck 1997. Modeling the Galileo dust measurements at Jupiter. *J. Geophys. Res.* **24**, 2175–2175.

Horanyi, M., G. Morfill, and E. Grün 1993a. Mechanism for the acceleration and ejection of dust grains from Jupiter's magnetosphere. *Nature* **363**, 144–146.

Horanyi, M., G. Morfill, and E. Grün 1993b. The dusty ballerina skirt of Jupiter. *J. Geophys. Res.* **98**, 221–245.

Krüger, H., E. Grün, D. P. Hamilton, M. Baguhl, S. Dermott, H. Fechtig, B. A. Gustafson, M. S. Hanner, M. Horanyi, J. Kissel, B. A. Lindblad, D. Linkert, G. Linkert, I. Mann, J. A. M. McDonnell, G. E. Morfill, C. Polanskey, R. Riemann, G. Schwehm, R. Srama, and H. A. Zook 1999a. Three years of Galileo dust data II. *Planet. Space Sci.* **47**, 85–106.

Krüger, H., E. Grün, A. Heck, and S. Lammers 1999b. Analysis of the field of view of the Galileo dust detector with collimated jovian dust streams. *Planet. Space Sci.* **47**, 159–172.

Krüger, H., A. V. Krivov, D. P. Hamilton, and E. Grün 1999c. Discovery of an impact generated dust cloud of Ganymede. *Nature* **399**, 558–560.

Zook, H. A., E. Grün, M. Baguhl, D. P. Hamilton, G. Linkert, J.-C. Liou, R. Forsyth, and J. L. Phillips 1996. Solar wind magnetic field bending of jovian dust trajectories. *Science* **274**, 1501–1503.